A New Class of Bullet Proof Materials: NanoComposites for Ballistic Applications

Antonio F. Ávila, Moises C. Andrade, Diego T. L. Cruz, Eder C. Dias, Douglas G. Sousa
Universidade Federal de Minas Gerais, Department of Mechanical Engineering, 6627 Antonio Carlos Avenue, Belo Horizonte - MG

***Abstract* — This paper focuses on ballistic tests of a new class of composite materials. The two hybrid nanocomposites studied are fiber glass epoxy nanoclay and nanographite. The fiber glass used is a plain weave 220 g/m^2, while the nanoclay (Nanomer I30E) and the nanographite (HC 11-IC). Ballistic tests were performed considering two types of ammunition, i.e. 38 caliber and 9 mm full metal jacketed. The results showed that for a 38 ACP e a 5 mm thick nanocomposite was able to absorb the energy efficiently. A 9 mm projectile was blocked by a two plate (5 mm each) arrangement with elastic deformation of the second plate less than 18 mm. The energies during the ballistic tests ranged from 315 to 576 joules.**

***Keywords* — Nanocomposites, Ballistic Tests, Nanographite, Nanoclay .**

I. INTRODUCTION

Ballistic materials have been studied for years especially for military applications. However, after the 9/11 and Madrid terrorist attacks, the usage of these materials became a valuable commodity even for the ordinary citizen. Another aspect is the great increase of bullet proof vehicles in large cities such as São Paulo and Mexico City due to the increase on urban violence. According to Caprino et al. [1], the Concorde tragedy occurred in Paris in 2000, was probably caused by a tire fragment moving at high speed and impinging the jet's fuel tanks. This is just another event that highlights the importance of the impact behavior of aeronautical materials. Langdon et al. [2] also argued that a fiber-metal laminate luggage container was capable of withstanding a bomb blast greater than that in the Lockerbie air disaster. According to Mines et al. [3], for high velocity impact, the perforation mechanics depend on the fiber type and volume fraction, the matrix, the stacking sequence, the size and initial kinetic energy of the impactor. Moreover, Cheng et al. [4] demonstrated that the penetration process can be broken down into three sequential stages: (i) punching; (ii) fiber breaking; and (iii) delamination. The authors even tried to model the perforation phenomenon by considering a failure criteria based into these three stages. Gu [5] went further by adding the composite strain energy to his model. He was able to simulate the progressive damage and delamination caused by the high velocity impact. Potti and Sun [6], however, considered the use of the dynamic response model along with the critical deflection criterion to analyze the high velocity impact and perforation. They concluded that the delaminated area increases with the velocity up to the penetration ballistic limit. However, beyond this limit, the delamination area decreases with the increase of velocity. By analyzing high velocity impact tests, Abrate [7] concluded that compressive strain in composites and the stress wave propagation through the thickness are related. Findik and Tarim [8] suggested the usage of aluminum substrate and composite materials as another option to steel products. Following the same approach, Villanueva and Cantwell [9] investigated the performance of fiber-metal laminates (FML) as skins of sandwich materials under high velocity impact conditions. They concluded that the application of aluminum foams associated to FML performed very well up to 120 joules. However, as stated by Findik and Tarim [8], the impact energy from fire arms ranges from low 700 joules from a 9 mm parabellum to high 2500 joules from a 7.62 caliber M1-rifle. Those values are far from the gas gun used by Villanueva and Cantwell.

An option to FML is the dispersion of nanoparticles into laminate composites, in special with epoxy systems. Yasmin et al. [10] were among those researchers who studied the effect of nanoparticles (organically modified montmorillonite - Cloisite 30B) into epoxy systems. By varying the amount of Cloisite 30B, in weight from 1% up to 10%, they observed an increase in the elastic moduli to a maximum of 80%. Another set of experiments on epoxy-nanoclay systems were conducted by Ho et al. [11]. They concluded that both stiffness and toughness were enhanced by the use of nanoparticles. However, for their binary system, resin - diglycidyl ether of bisphenol *A* and cure agent - triethylenetetramine, the ultimate tensile strength was obtained at 5% in weight of montmorillonite content. Consistent with Ho et al. [11], Ávila et al. [12] not only reported an increase on ultimate strength for 5% content of montmorillonite, in their case Nanomer I30E from Nanocore Inc., but they also pointed to an increase on impact resistance close to 48%. By impact resistance Ávila et al. [12] meant the composite capacity of absorb energy without a catastrophic failure.

The objective of this paper is to study the high velocity impact response of a polymer-nanoclay-fiber glass nano-structured laminate, where the heating phase is not present.

II. EXPERIMENTAL PROCEDURE

A. Materials

The hybrid nanocomposites were manufactured following the procedure described in Ávila et al. [12]. A plain weave fiber

Antonio F. Ávila, aavila@netuno.lcc.ufmg.br, Tel. + 55 31 3409-5238, FAX. + 55 31 3443-3783. This work was funded by the Brazilian Research Council - CNPq granst 300826/2005-2 and 550067/2005-1.

glass with 220 g/m^2 aerial density was used as traditional reinforcement. The epoxy formulation was based on *diglycidyl ether of bisphenol A* resin and a hardener, *triethylenetetramine*. The matrix nano-reinforcement was made by mechanical mixing. Two types of nanoparticles, i.e. nanoclay and nanographite, were employed. The nanoclay was an organically modified montmorillonite (MMT) in a platelet form, i.e. 10 μm long, 1 μm wide and 50 *n*m thick, called Nanomer I30E from Nanocor, while the nanographite (HC 11-IC) was supplied by Nacional Grafite. A dispersant agent, acetone, was employed to improve the mixing process. The degassing stage was required to eliminate bubbles generated during the mechanical mixing and to eliminate the dispersant agent, i.e. acetone. After this procedure, the hand lay-up with vacuum assisted cure was performed. From previous experiments, the largest amount of nanographite dispersed into the epoxy system without phase separation was 3 %wt. Therefore, for this study this value was adopted. Consistent with Ávila et al. [12], the amount of nanoclay employed was 5 %wt. Moreover, the fiber/epoxy ratio was kept constant and equal to 65%. Each 5 mm thick square plate with 32 layers prepared was 0.35 m wide and 0.35 m long.

B. Ballistic Tests

The ballistic tests were performed according to NIJ standard 0101.03 [13] for a type I and II-A classifications. The target was hold by a steel frame which provided a clamped condition for all four edges. It is worth to mention that a rectangular container holding 50 kilograms plasticine at 37 C was placed right behind the target/frame to simulate the human body as described by NIJ standard. Two different projectiles were used for this investigation. The first one was the 38 caliber special (38 SLP), standard ammunition used by most of the Brazilian Police Departments. The second type of ammunition was a 9 mm full metal jacket (9 mm FMJ), used by the Brazilian Armed Forces. The 38 SLP projectile has a mass of 10.2 grams, while the 9 mm FMJ has a mass of 7.45 grams. For the 9 mm FMJ projectile the lead projectile is covered by a copper shell for improvement of aerodynamic and impact performances. Another important difference between the two ammunitions is their average velocity, i.e. 220 m/s and 380 m/s for 38 SLP and 9 mm FMJ, respectively. Table I indicates the type of ammunition employed for each ballistic test as well as their weight, speed and impact energy.

C. Damaged Area and Residual Bending Strength

For ballistic applications, where different impact regions are located at same target, a different methodology has to be applied. Instead of evaluating the residual compression strength; the proposed methodology focused on the residual bending strength. This methodology is based on the formation of ballistic cone as described by Naik and Shrirao [14] during the high velocity impact tests. Moreover, the residual bending properties are dependent on the damage extension and its location. Following Silva Jr et al. [15], the damage extension has to be evaluated by the ratio between the back and front damaged areas, a non-dimensional parameter defined as $\eta = BA/FA$. In addition to η parameter, another non-dimensional parameter (ξ) is also defined, i.e. $\xi = D/(L/2)$, where D is the distance between the bending force application location and the damaged area center of mass, while $L/2$ is the specimen semi-length. Notice that ξ is defined in such way when $\xi \rightarrow 0$; this means that the bending residual strength also leads to zero. Furthermore, when $\xi \rightarrow 1$, the bending properties are similar to the undamaged specimen properties.

TABLE I. PROJECTILES INFORMATION

Test	Projectile Characteristics			
	Type	Mass [g]	Speed [m/s]	Energy [J]
1	9 mm FMJ	8.0	379.48	576.02
2	38 SLP	10.2	244.75	305.50
3	38 SLP	10.2	247.80	313.17
4	9 mm FMJ	8.0	379.48	576.02
5	38 SLP	10.2	246.28	309.34
6	9 mm FMJ	8.0	376.74	567.73
7	38 SLP	10.2	248.72	315.49
8	9 mm FMJ	8.0	373.08	556.76
9	9 mm FMJ	8.0	333.75	445.56
10	9 mm FMJ	8.0	332.54	442.33
11	9 mm FMJ	8.0	333.45	444.76
12	9 mm FMJ	8.0	335.28	449.65
13	38 SLP	10.2	234.09	279.47
14	38 SLP	10.2	244.14	303.98
15	38 SLP	10.2	243.23	301.72
16	38 SLP	10.2	235.92	283.86

Eight different targets configurations where studied and their properties are summarized in Table II. As described early, six shots were performed for each plate. Once the ballistic tests were performed, the damaged areas were measured by image processing using the public domain software ImageJ 1.37. From each plate, at least 6 bending specimens (50 mm wide x 350 mm long and 5 mm thick) were prepared and tested following the ASTM D 790 standard [13].

TABLE II. TARGET CHARACTERISTICS

Target ID	Target Characteristics
P2	MMT 5%+1 layer of MMT 25%
P3	MMT 5%+3 layers of MMT 25%
P4	MMT 5%+1 layer of MMT 33%
P5	Pure fiber glass/epoxy
P6	MMT 5%
P9	Pure fiber glass/epoxy
P10	MMT 5%
P11	Nanographite 3%

III. DATA ANALYSIS

Tables III and IV summarize the data obtained after each fire test. Each damaged area was measured by image processing technique; at least 6 measurements were performed. The delaminated area, back (BA) and front (FA), and the back elastic deformation (BED) were measured. In most cases three distinct damaged areas were noticed on back area, while two different regions, i.e. projectile impact and delamination areas were observed. The occurrence of perforation was also detected. From Tables III and IV, it is possible to conclude

that there is an increase on delamination with the presence of nanoparticles, i.e. nanoclay and graphite nanoflakes. According to Silva Jr. et al. [15], the delamination failure is the most common mechanism of energy absorption. In this investigation, the μ parameter reached the 12.84 mark, an indication of good performance. Furthermore, when the two plates are associated in series, i.e. cases 8-12, the results are very good. Yet, despite of the large vales of μ, in two cases the perforation was noticed. This phenomenon suggests that not only the delamination mechanism is present during the impact event.

TABLE III: BALLISTIC TEST RESULTS

Test ID	Plate ID	BED [mm]	Perforation
1	P3	-----	YES
2	P3	5.0	NO
3	P2	7.5	NO
4	P2	-----	YES
5	P4	8.0	NO
6	P4	-----	YES
7	P5	13	NO
8	P5+P6	16	NO
9	P9+P10	13	YES
10	P9+P10	16.2*	YES
11	P9+P11	17.0*	YES
12	P9+P11	8.2	NO
13	P10	-----	YES
14	P10	7.9	NO
15	P11	14.0	NO
16	P11	11.5	NO

* Damaged cone measured

TABLE IV. DAMAGED AREAS, Λ AND M VARIABLES

ID	BA[mm^2]	FA[mm^2]	μ	λ
1	2811.94±41.23	771.35±42.32	3.65±0.15	0.486
2	10899.12±43.79	1340.85±44.74	8.14±0.23	0.592
3	5586.71±29.63	501.38±20.14	11.16±0.39	0.514
4	3921.74±30.69	2652.18±43.33	1.48±0.01	0.383
5	4993.56±18.67	6866.08±16.72	0.73±0.01	0.457
6	5158.38±39.44	2893.93±11.59	1.78±0.06	0.314
7	3761.95±25.81	4345.73±66.51	0.87±0.01	0.240
8*	3103.29±38.64	550.02±38.53	5.67±0.33	0.286
	5295.82±38.09	4431.03±28.74	1.19±0.01	
9*	2962.22±58.58	231.29±3.93	12.84±0.03	0.142
	3286.00±47.76	2395.15±48.07	1.37±0.08	
10*	1388.82±16.25	231.29±3.93	6.01±0.03	0.371
	1849.23±77.19	1175.53±24.77	1.57±0.03	
11*	1032.23±10.08	231.30±3.93	4.46±0.03	0.429
	3086.22±31.12	1029.95±15.64	2.99±0.01	
12*	1215.46±17.04	231.32±3.92	5.26±0.02	0.657
	3090.33±15.73	1329.92±60.37	2.33±0.09	
13	2118.21±43.94	1681.25±61.11	1.26±0.02	0.771
14	3528.30±95.25	2394.23±46.71	1.47±0.01	0.800
15	2962.69±30.51	1825.87±24.79	1.62±0.01	0.171
16	2616.69±34.91	1518.31±42.98	1.72±0.03	0.714

* Plate position according to table 3

The ballistic cone formation due to the projectile compression on target, mentioned by Naik and Shrirao [16], can be the cause another failure mechanism presence. When the ballistic cone is formed, in addition to the local compressive loading, a bending stress is also applied, mainly into the surrounding areas of the projectile impact. Tension and compression loading are developed through the composite thickness. Micro-buckling, due to the compression stresses developed during the bending can be the cause of failure into the fibers close to the internal region (front area). At same time, fiber breakage is occurring due to tension on the back area. Such mechanism also leads to delamination due to the shear stress generated between layers.

In their study, Naik and Shrirao [16], did not considered the projectile deformation as a source of damage inside the composite. Figure 1 shows the case where the 38 caliber projectile after penetration of some layers "spread" between layers. In this case, the μ parameter, indicates a low performance, as its value is low. However, due to the nature of the damage, the μ parameter is not enough to evaluate the ballistic performance. The back elastic deformation and the perforation condition must be considered. Furthermore, by analyzing the BED (≈ 13 mm) and perforation condition, according to the NIJ standard [13], the composite performance is acceptable.

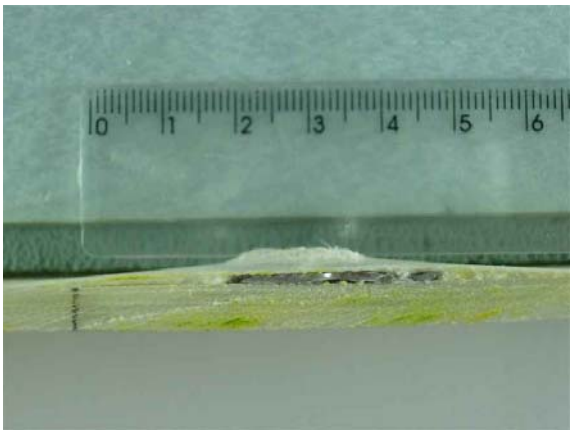

Fig 1. 38 caliber impact in a fiber glass/epoxy

A different behavior has noticed when the amount of nanoclay was increased on the front area, e.g. case P4. During the 38 caliber impact on a P4 nancomposite the projectile hits the plate and rebounds. Such fact can be attributed to the nanoclay layer. However, this rebound also caused an extensive damage as shown in Fig. 2.

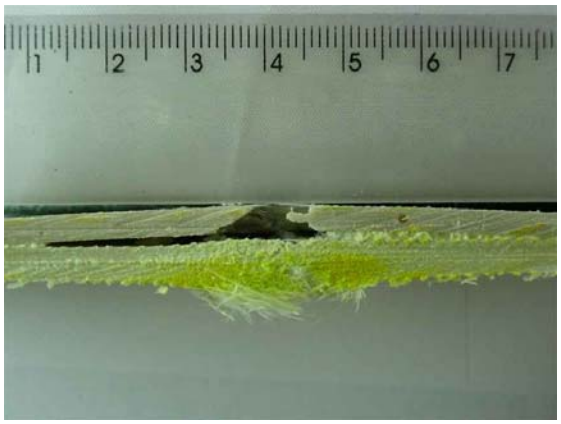

Fig. 2. 38 caliber impact in a P4 nanocomposite

The 9 mm FMJ impact also was affected by the nanoclay/graphite nanoflakes presence. Figures 3-4 show the failure mechanism in these cases. The extra nanoclay layer disbanded from the fiber glass/epoxy/nanoclay part when the number of layers increased from 1 (P2 condition) to 3 (P3

condition), or the amount of nanoclay increased from 25% (P2) to 33% (P4). Such fact can be attributed to the local increase on stiffness, which creates "a shield" for the laminate.

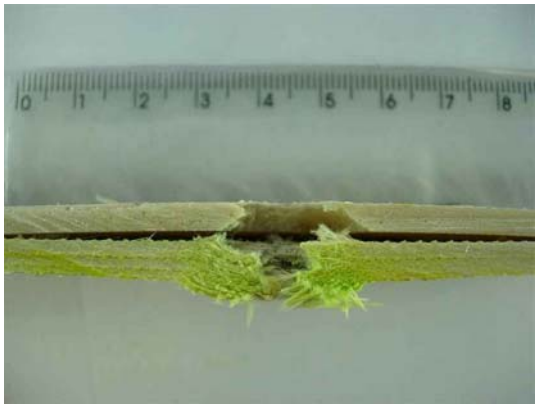

Fig. 3. 38 caliber impact in a P3 nanocomposite

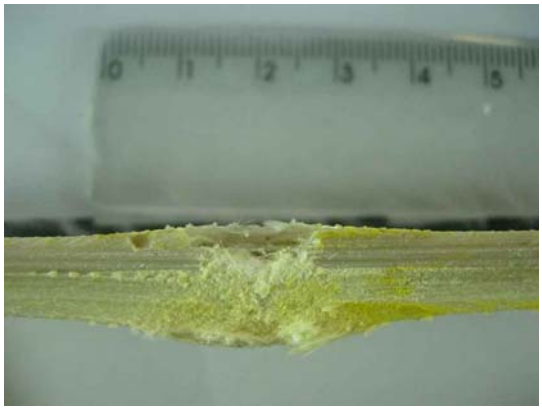

Fig.4 9 mm FMJ impact in a P2 nanocomposite

The addition of nanoclay and graphite nanoflakes has direct influence on high velocity impact resistance of laminate composites. However, the failure mechanisms and damage generated is also dependent of the amount of such nanoparticles disperse, how they are dispersed and the ammunition used during the ballistic tests. Due to the nature of graphite nanoflakes, another hypothesis can also be formulated. The presence of nanoparticles increases the friction coefficient between projectile and target, inducing an addition deformation to the bullet and increasing the energy absorption. Figure 6 shows a transverse cut of a P11 plate. Notice that in this case the 9 mm projectile was trapped inside the damage area.

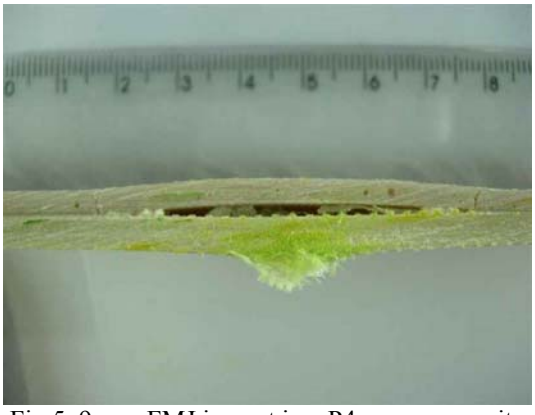

Fig.5. 9 mm FMJ impact in a P4 nanocomposite

The different failure mechanisms are consequence of the type of target tested and the ammunition used, as shown in Figure 7. However, the usage of nanoparticles, nanoclays or graphite nanoflakes, seems to be a valuable addition to the composite. Notice that nanoparticles/nanoflakes have direct effect on composite strain rates, as demonstrated by the SHPB tests in Ávila et al. [17]. Moreover, the bending strength is also affected by the nanoparticles addition to the composite.

Fig. 6. 9 mm trapped inside the damage area

Fig. 7. Bullets after impact

Finally, this behavior can be explained by the nanostructures formed inside the matrix. Figure 8 described this type of nanostructures.

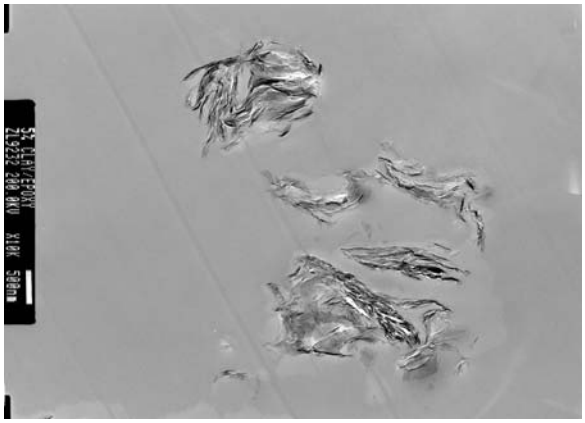

Fig 8. TEM analysis

By analyzing Figure 9, it is possible to conclude that X-ray diffraction (XRD) tests revealed that rather than exfoliated into the epoxy system, the MMT nanoclay was in the

intercalated form. Another important issue that must be addressed is the matrix saturation limit regarding the nanoclay content. The basal spacing calculated using Bragg's law indicates an increase from 1.35 nm to 1.38 nm when the nanoclay content changed from 5 wt% to 10 wt%. Yet, the amount of nanoclay is twice as much for the 10 wt% nanoclay content specimens and the XRD intensity increases only 57%.

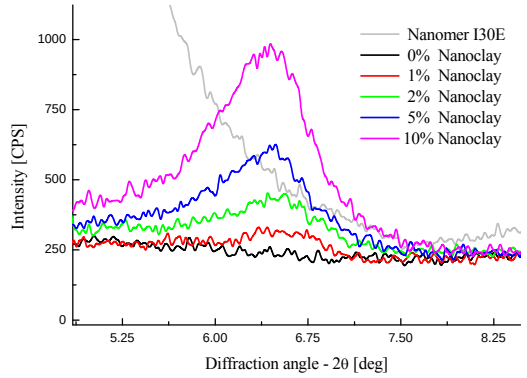

Fig. 9 XRD signature.

By analyzing Figure 9, it is possible to conclude that X-ray diffraction (XRD) tests revealed that rather than exfoliated into the epoxy system, the 30B nanoclays were in the intercalated form. Another important issue that must be addressed is the matrix saturation limit regarding the nanoclay content. The basal spacing calculated using Bragg's law indicates an increase from 1.35 nm to 1.38 nm when the nanoclay content changed from 5 wt% to 10 wt%. Yet, the amount of nanoclay is twice as much for the 10 wt% nanoclay content specimens and the XRD intensity increases only 57%. This unexpected reduction on the diffraction intensity is an indication of a disordered swollen structure, as demonstrated by Fan et al. [17]. Likewise, Ranade et al. [18] stated that it could be an evidence of a small amount of nanoclay that does not get exfoliated or intercalated, but remains in its own identity leading to an immiscible nano system. This seems the case for the 10 wt% concentration samples. This hypothesis can be visualized in Figures 8 and 9 where the presence of these immiscible nano systems clusters (white regions) and an intercalated nanostructure can be observed. As stated by Avila et al. [12] a partially exfoliated/intercalated system is most likely to occur due to the dispersion system used. In summary, they believed that dispersion process is controlled not only by the nanoparticle morphology but it is also affected by the manufacturing process, e.g. direct mixing, shear mixing, and sonication.

IV. CONCLUSIONS

The addition of nanoclay and nanographite to fiber glass/epoxy laminates not only increases the high velocity impact resistance of these composites, but it also has influence on their failure mechanism. The residual bending strength increases approximately 32 % with the addition of 5% in weight of nanoclay. The addition of 3% in weight of nanographite represented an improvement close to 30% on residual bending strength. The failure mechanism also changed with the addition of nanoparticles. The nanoclay addition to the hybrid nanocomposite represented an increase on delamination, i.e. 68% and 2930% for the front and back sides, respectively.

The nanographite effect can also be translated as a large increase on delamination process. Although the front side impacted delaminated area seems to be approximately the same, the back side delaminated area enlarged by 557%. In both cases, the delamination process seems to be predominant.

The average lower bound energy absorption for the hybrid nanocomposite seems to be around 313 Joules. For the sandwich configuration (two plates associated back to back) the lower bound energy absorption can be placed between 450 and 556 Joules. Following the NIJ standard, it is possible to classify these nanocomposites as an armor type I for a 5 mm thickness and a type II-A when the thickness is equal to at least 10 mm, as the maximum back elastic deformation measured, i.e. 16 mm, was less than 38 mm (1.5 inches).

REFERENCES

[1] G. Caprino, V. Lopresto and D. Santoro. "Ballistic impact behavior of stitched graphite/epoxy laminates", *Comp. Sci. and Technology*, vol. 67, pp. 325-335, Jan. 2007.

[2] G.S. Langdon, SI. Lemarski, GN Nurick, MC Simmons, WJ. Cantwell, and GK. Scheleyer, "Behavior of fibre-metal laminates subjected to localized blast loading: Part I – Experimental observations", *Int. J. of Impact Engineering*, vol. 34, pp. 1202-1222, Aug. 2007.

[3] RAW. Mines, AM. Roach, and N. Jones, "High velocity perforation behavior of polymer composite laminates", *Int. J of Impact Engineering*, vol. 22, pp.:561-588, July 1999.

[4] WL. Cheng, S. Langlie, and S. Itoh, S. "High Velocity Impact of Thick Composites", *Int. J of Impact Engineering*, vol. 29, pp. 167-184, Jan. 2003.

[5] B. Gu, "Analytical modeling for ballistic perforation of planar plain-woven fabric target by projectile", *Composites Part B*, vol. 34, pp. 361-371, Feb. 2003.

[6] SV. Potti,. and CT. Sun, " Prediction of impact Induced Penetration and Delamination in Thick Composite Laminates, *Int. J of Impact Engineering*, vol. 19, pp. 31-48, Jan. 1997.

[7] S. Abrate *Impact on Composite Structures*, Cambridge: Cambridge UP, 1998, pp. 50-111.

[8] F. Findik, and N. Tarim, N. "Ballistic impact efficiency of polymer composites", *Composite Structures*, vol. 6, pp. 187-192, Jan. 2003.

[9] GR. Villanueva, and WJ. Cantwell, "The High Velocity Impact Response of Composite and FML-Reinforced Sandwich Structures", *Comp. Sci. and Technology,* vol. 64, pp. 35-54, Jan. 2004

[10] A. Yasmin, J-J. Luo, and IM. Daniel, Processing of Graphite Nanosheet Reinforced Polymer Nano composites, *Proceedings of the 19th ASC/ASTM Joint Technical Conference*, Georgia: ASC, CDROM, 2004.

[11] M-W. Ho,C-K. Lam, K-T Kau, DHL. Ng, and D. Hui, "Mechanical properties of epoxy-based composites using nanoclays", *Composites Structures*, vol. 75, pp. 415-421, March 2006.

[12] AF. Ávila, MI. Soares, and A. Silva Neto, "A study on nanocomposites laminated plates behavior under low velocity impact", *Int. J. of Impact Engineering*, vol. 31, pp. 28-41, Jan. 2007.

[13] NIJ Standard 0101.03 "Ballistic resistance of police body armor", *U.S. Department of Justice, National Institute of Justice*, Washington DC, pp 1-13, 1987.

[14] N.K. Naik, P. Shrirao, and BCK Reddy, "Ballistic Impact Behavior of Woven Fabric Composites: Formulation, *Int. J. of Impact Engineering*, vol. 32, pp. 1521-1552, Oct. 2006.

[15] JEL. Silva Junior, S. Paciornik, and JRM. d'Almeida, "Evaluation of effect of ballistic damaged area on the residual impact strength and tensile stiffness of glass-fabric composite materials", *Composite Structures*, vol. 64, pp. 123-127, Jan. 2004.

[16] NK. Naik, and P; Shrirao, "Composite structures under ballistic impact", *Composite Structures*, vol. 66, pp. 578-590, Aug. 2004.

[17] X Fan, C. Xia, and RC. Advincula, "Intercalation of Polymerization Initiators into Montmorillonite Nanoparticle Platelets: Free Radical vs. Anionic Initiator Clays," *Colloids and Surfaces A: Physicochem. Eng. Aspects,* vol. 219, pp. 75-86, Jan. 2003.

[18] A. Ranade, NA. D'Souza, and B. . Gnade, B. "Exfoliated and intercalated polyamide-imide nanocomposites with montmorillonite," *Polymer*, vol. 43, pp.3759-3766, Oct. 2002.